Effect of Fe substitution on the magnetic ordering in $Ca_3(Co_{1-x}Fe_x)_2O_6$

I. Nowik,[1] A. Jain,[2] S. M. Yusuf,[2] and J. V. Yakhmi[3]
[1]*Racah Institute of Physics, The Hebrew University, Jerusalem 91904, Israel*
[2]*Solid State Physics Division, Bhabha Atomic Research Centre, Mumbai 400085, India*
[3]*Technical Physics and Prototype Engineering Division, Bhabha Atomic Research Centre, Mumbai 400085, India*
(Received 4 July 2007; revised manuscript received 21 October 2007; published 4 February 2008)

Mössbauer studies over 4.2–550 K of iron doped quasi-one-dimensional spin chain compounds $Ca_3(Co_{1-x}Fe_x)_2O_6$, crystallizing in rhombohedral structure (space group $R\bar{3}c$) for $x \leqslant 0.2$, reveal that the iron resides only in the Co2 (6*a*) site. The compounds are paramagnetic at 90 K, and the iron exhibits slow spin relaxation phenomena even at room temperature. However, for the $x=0.5$ compound, the crystal structure is triclinic ($P\bar{1}$), and the iron resides almost equally in two different crystallographic sites and exhibits a very high magnetic ordering temperature $T_N \sim 500$ K. Both iron sites exhibit quadrupole interactions of almost equal size; however, with opposite sign $\left(\frac{1}{4}e^2qQ \approx \pm 0.62 \text{ mm/s}\right)$. At $T_{sr}=193$ K, a spin reorientation of the iron magnetic moments is observed. Below 150 K the magnetic moments are tilted at 20° relative to the local electric field gradient axis and above 230 K they are aligned perpendicular to this axis. These results agree well with magnetic susceptibility measurements, in which a sharp drop in magnetization is observed above 200 K. The magnetic hyperfine fields in the two sites at 4.2 K are 53.3 and 45.7 T, respectively. The net magnetic interaction is antiferromagnetic, however, with a small ferromagnetic component displaying hysteresis along with a saturation magnetization of about $0.02\mu_B$/f.u. at 1.5 K.

DOI: 10.1103/PhysRevB.77.054403 PACS number(s): 76.80.+y, 61.05.cp, 75.30.Cr, 76.60.Es

I. INTRODUCTION

The compound $Ca_3Co_2O_6$ with K_4CdCl_6-type crystal structure (space group $R\bar{3}c$) has quasi-one-dimensional spin chains, which are made up of alternating face-sharing CoO_6 octahedra (Co1) and CoO_6 trigonal prisms (Co2) arranged along the hexagonal *c* axis. The Co ions at both sites are in trivalent oxidation state, but due to the different crystalline electric fields they are in the different spin states [high spin state ($S=2$) at the trigonal prism site and low spin state ($S=0$) at the octahedral site]. The important features[1–11] of this compound are ferromagnetic intrachain and antiferromagnetic interchain interactions. The magnetic properties of iron doped compounds, namely, $Ca_3(Co_{1-x}Fe_x)_2O_6$ ($x \leqslant 0.2$), have been studied in the literature[12,13] and also by some of us.[1] The major conclusion was that the substitution of iron for Co, occupying the Co2 site, weakens the one-dimensional character of the Co-Co exchange interactions, and introduces much stronger Fe-Fe intrachain and interchain exchange interactions. Here we present the results of x-ray diffraction, dc magnetization, and Mössbauer spectroscopy studies of iron doped compounds $Ca_3(Co_{1-x}Fe_x)_2O_6$ ($x=0.1$, 0.2, and 0.5) to investigate the magnetic properties of these Fe substituted samples. The present study shows that for the compounds with $x \leqslant 0.2$, the crystal structure is rhombohedral (space group $R\bar{3}c$). These compounds show a paramagnetic behavior at 90 K along with slow spin relaxation phenomena for iron even at room temperature. The results of x-ray diffraction study show that for the highest concentration of Fe, i.e., for the compound Ca_3CoFeO_6, the crystal structure has changed to triclinic (space group $P\bar{1}$). Due to the change of crystal structure, the magnetic properties of this $x=0.5$ compound are very much different from the compounds with $x \leqslant 0.2$. It is found that the compound Ca_3CoFeO_6 orders magnetically much above room temperature ($T_N \sim 500$ K) and displays a spin reorientation transition at ~193 K.

II. EXPERIMENTAL DETAILS

The polycrystalline samples of $Ca_3(Co_{1-x}Fe_x)_2O_6$ ($x=0.1$, 0.2, and 0.5) were prepared by the conventional solid state reaction method as described earlier.[1] Powder x-ray diffraction (XRD) measurements were performed on all the three samples at room temperature using the Cu $K\alpha$ radiation from scattering angle (2θ) 10° to 90° in equal 2θ steps of 0.02°. The magnetization measurements were carried out using a commercial (Oxford Instruments) vibrating sample magnetometer. The Mössbauer study was performed using a conventional constant acceleration drive, a 50 mCi ^{57}Co: Rh source, and absorbers, putting in perspex holders for low temperatures (4.2–300 K) and in boron nitride holders for high temperature measurements (300–520 K). The velocity calibration was done with a room temperature α-Fe absorber. The experimentally observed spectra were least square fitted with calculated spectra according to various models. The spectra for the $x=0.1$ and 0.2 samples, at 90 and 300 K, were fitted in terms of spin up-down relaxation theory formulas.[14] The spectra for the $x=0.5$ sample were analyzed in terms of full diagonalization of the Hamiltonian of magnetic and quadrupole interactions, where the magnetic field is at an angle θ relative to the local axis of the electric field gradient (EFG), for simplicity, assuming axial symmetry for two different sites of iron.

III. EXPERIMENTAL RESULTS AND DISCUSSION

Rietveld analysis of the x-ray diffraction patterns for the compounds $Ca_3(Co_{1-x}Fe_x)_2O_6$ ($x=0.1$ and 0.2) confirms the single phase formation in the rhombohedral structure (space

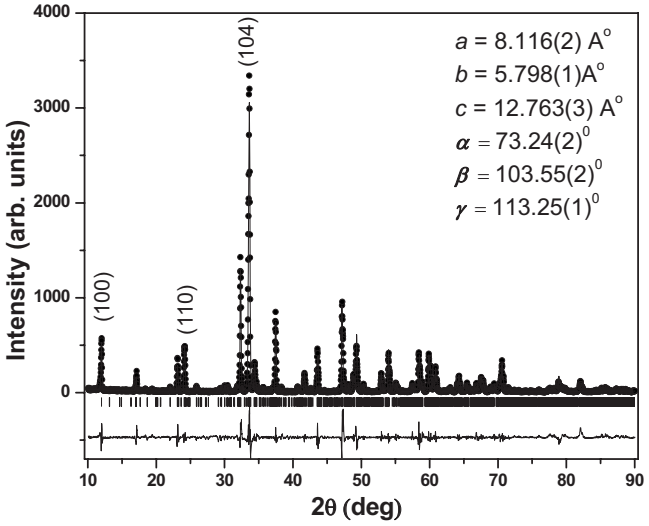

FIG. 1. The x-ray diffraction pattern for Ca_3CoFeO_6. The solid line at the bottom of the figure shows the difference between the observed and the calculated patterns.

group $R\bar{3}c$) as already reported.[1] The profile matching refinement of the x-ray diffraction pattern for Ca_3CoFeO_6 ($x=0.5$), using the WINPLOTR,[15] shown in Fig. 1, confirms the formation of a single phase, in the triclinic structure (space group $P\bar{1}$). The unit cell parameters are shown in the figure panel. The c axis is at angle of $18.47 \pm 0.04°$ relative to the perpendicular to the a-b plane. The unit cell volume is 523.3 $Å^3$. It may be mentioned here that the used profile matching refinement method[15] allows one to obtain only the name of the crystal system, its space group, and the lattice parameters. Since with the highest Fe substitution ($x=0.5$) the crystal structure has completely changed from the known rhombohedral structure (for lower Fe substituted samples), it is not possible to use the Rietveld refinement method which needs position of all the atoms in the unit cell. Hence the used method, unlike the Rietveld profile refinement, does not give the refined position of the atoms in the unit cell. Hence, we are not in a position to give any further structural details. However, the present diffraction data analysis could clarify the single phase nature of the sample with the above mentioned crystallographic information. Our Mössbauer study clearly shows that the Fe atoms occupy two different crystallographic sites.

The Mössbauer spectra for the $x=0.1$ and 0.2 samples (Fig. 2) were analyzed in terms of the spin relaxation theory,[14] and it yields perfect fits in terms of χ^2 values, and confirms the earlier conclusions[1] that the iron occupies only one site (Co2), with a negative quadrupole interaction, $EQ = \frac{1}{4}e^2qQ$ (=−0.62 mm/s at 90 K). The analysis also yields (assuming a fluctuating magnetic hyperfine field of 45 T) the room temperature spin relaxation rates, which are 1.5×10^{11} and 7.7×10^{10} s^{-1} for $x=0.2$ and $x=0.1$, respectively, indicating the dominance of Fe-Fe spin-spin relaxation. The ratio of the relaxation rates (~2) equals the ratio of iron concentration, expected for spin-spin relaxation. Also the fact that the $x=0.2$ sample at 90 K exhibits a spectrum with a relaxation rate of 5.5×10^{10} s^{-1}, not very much smaller

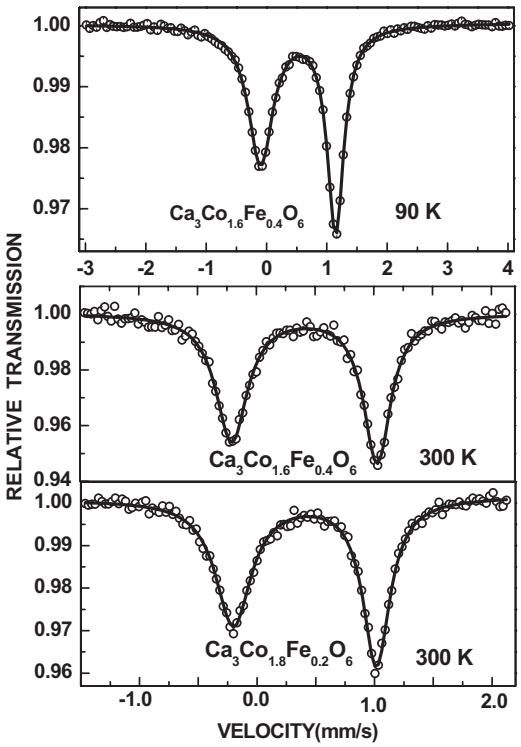

FIG. 2. The Mössbauer spectra of $Ca_3(Co_{1-x}Fe_x)_2O_6$ for the $x=0.1$ and 0.2 samples.

than that at 300 K, indicates the dominance of the spin-spin relaxation process. The relaxation rate certainly does not follow a high temperature power law expected for spin-lattice relaxation.

The $x=0.5$ sample, Ca_3CoFeO_6, exhibits spectra displaying magnetic order up to 500 K. Spectra were recorded at temperatures ranging from 4.2 to 520 K. Some of the spectra are displayed in Figs. 3 and 4. Just by counting the number of absorption lines in the spectra (Fig. 3) it is obvious that they are composed of two Fe subspectra of different crystallographic sites. The one with the larger hyperfine field, larger isomer shift, and positive qaudrupole interaction is denoted arbitrarily as site 1. Table I depicts the parameters that are obtained from the analysis of the spectra in terms of full diagonalization of the Hamiltonian of magnetic and quadru-

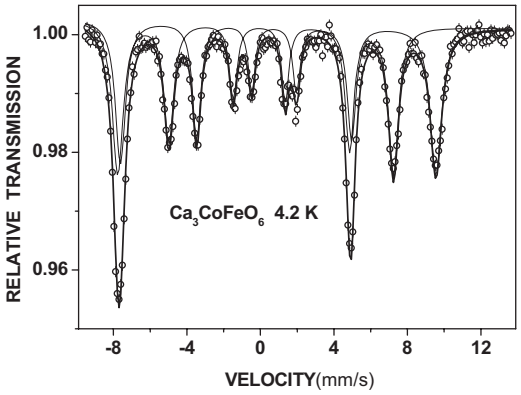

FIG. 3. The Mössbauer spectrum of Ca_3CoFeO_6 at 4.2 K.

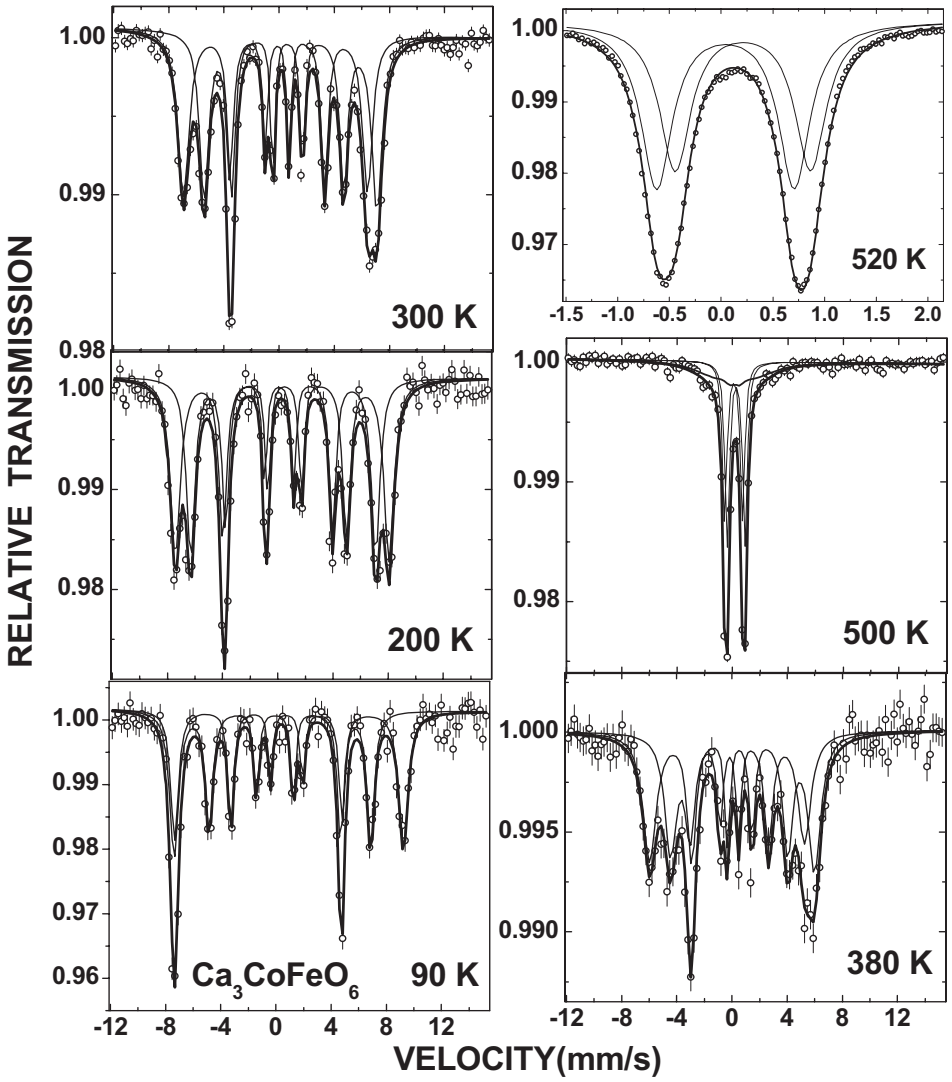

FIG. 4. The Mössbauer spectra of Ca_3CoFeO_6 at various temperatures.

pole interactions, where the magnetic field is at an angle θ relative to the axis of the EFG for two different crystallographic Fe sites. The solid lines in the figures show the least square fit simulated spectra. Figure 5 depicts the temperature dependence of the relative spectral areas under the two subspectra, giving approximately the relative occupation of Fe in the two sites. One observes that they are almost of equal intensity; the slight difference may be the result of a slightly

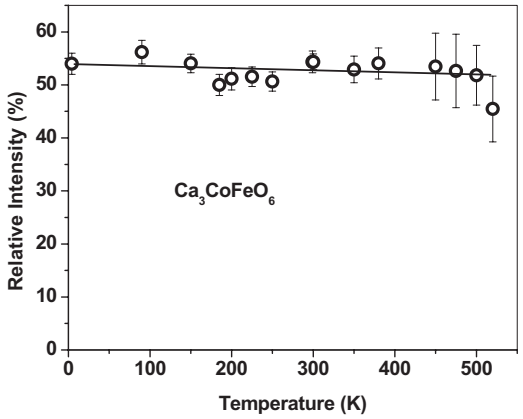

FIG. 5. The relative intensity of one of the subspectra of Fe ("1").

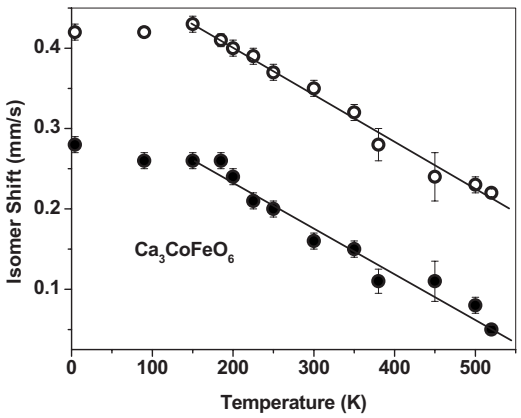

FIG. 6. The temperature dependence of the isomer shifts of the two Fe sites, ("1" open circles).

TABLE I. The parameters derived from the analysis of the Ca_3CoFeO_6 Mössbauer spectra. The error bars of these parameters are shown in the corresponding figures. The isomer shifts (IS1 and IS2) are relative to that of iron at room temperature. EQ1 and IN1 stand for the quadrupole interaction and the relative intensity of site "1."

Temp. (K)	IN1 (%)	IS1 (mm/s)	EQ1 (mm/s)	HF1 (T)	θ 1 (deg)	IS2 (mm/s)	EQ2 (mm/s)	HF2 (T)	θ 2 (deg)
4.2	54	0.42	0.68	53.3	25	0.28	−0.64	45.7	23
90	56	0.42	0.60	51.5	18	0.26	−0.64	43.7	20
150	54	0.43	0.60	49.9	29	0.26	−0.68	42.8	35
185	50	0.41	0.60	48.9	48	0.26	−0.61	42.2	51
200	51	0.40	0.59	48.0	61	0.24	−0.70	41.2	64
225	52	0.39	0.60	47.1	79	0.21	−0.73	40.5	80
250	51	0.37	0.62	46.0	82	0.2	−0.7	39.2	81
300	54	0.35	0.56	43.2	80	0.16	−0.67	36.3	85
350	53	0.32	0.54	40.3	90	0.15	−0.65	33.5	90
380	54	0.28	0.56	36.8	90	0.11	−0.62	29.7	90
450	53	0.24	0.56	28.6	90	0.07	−0.57	21.9	90
500	52	0.23	0.62	0		0.08	−0.65	0	
520	46	0.22	0.64	0		0.05	−0.65	0	

different recoil free fraction for the two sites. Thus it is clear that for this concentration of iron ($x=0.5$), the iron occupies two different crystallographic sites with almost equal probability. In Fig. 6, we show the temperature dependence of the isomer shift for the two sites. Except for the fact that the isomer shift is different for the two sites, there is nothing unusual in these behaviors, displaying the normal high temperature linear shift.

In Fig. 7, the temperature dependencies of the quadrupole interactions are shown. Here we observe a surprising result, the Fe quadrupole interaction in the two sites is almost equal in strength, yet of opposite sign. The quadrupole interactions change very little with temperature, as expected for an ionic Fe^{+3} ($S_{5/2}$ state), where the electric field gradient is due to lattice charges.

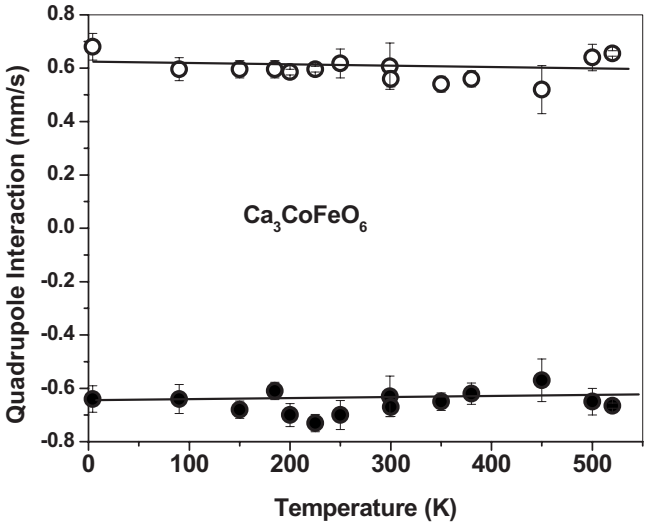

FIG. 7. The temperature dependence of the two quadrupole interactions in the two Fe sites ("1" open circles).

Figure 8 displays the temperature dependence of the two hyperfine fields. We observe that the hyperfine field for two different sites varies smoothly with temperature, the value of hyperfine field changing from 52 and 43 T, respectively, at low temperature to zero above 500 K. The solid lines in Fig. 8 represent the parameterless (except for the normalization of the fields to 52 and 43 T at low temperatures) pure spin 5/2 Brillouin functions, indicating almost identical temperature dependencies of the magnetic moments in the two sites. The spectrum at 520 K, shown in Fig. 4, was analyzed in terms of two pure quadrupole doublets. A very interesting result is displayed in Fig. 9, in which the temperature dependence of the angles θ_1 and θ_2 at which the hyperfine fields point relative to the local EFG axis are displayed. One observes that θ_1 and θ_2 are equal to each other and change drastically with temperature. While at low temperatures, below 150 K, the moments in both sites are aligned at an angle of $20\pm3°$ relative to the EFG axis, above 230 K they are perpendicular to the EFG axis. These results indicate that the axis of the

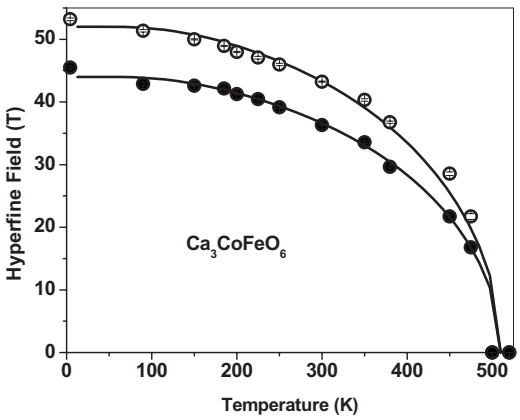

FIG. 8. The temperature dependence of the two hyperfine fields. The solid lines are pure spin 5/2 Brillouin functions.

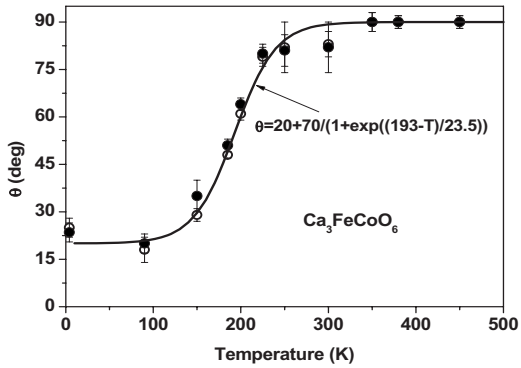

FIG. 9. The temperature dependence of the angles θ_1 and θ_2.

EFG in both sites is perpendicular to the unit cell basal plane (a-b plane) and at low temperatures the moments are probably along the unit cell c axis, which is at an angle of 18.5° relative to the perpendicular to the a-b plane, as obtained by the x-ray diffraction results shown in Fig. 1. At the high temperatures the magnetization lies in the basal plane. The solid line in Fig. 9 is a least square fit of the step function formula: $\theta=\theta_0+(90.0-\theta_0)/\{1.0+\exp[(T_{sr}-T)/W]\}$, yielding $\theta_0=20\pm3°$, $T_{sr}=193\pm5$ K, and $W=23\pm2$ K. The relative alignment of the magnetic moments for the two sites is depicted schematically in Fig. 10.

The temperature dependent dc magnetization curves in the temperature range 5–320 K are shown in Fig. 11. It is clear that the magnetic ordering temperature is above the highest recorded temperature. The zero field cooled and field cooled magnetization curves do not merge even at 320 K, in agreement with the Mössbauer studies. Around 200 K, one observes a sharp drop in magnetization, which can be associated with the spin reorientation found in the Mössbauer studies. The magnetic field dependence of magnetization at 1.5 K presented in Fig. 12 indicates that at high magnetic fields, the magnetization varies linearly with magnetic field, as expected for an antiferromagnet; however, a small ferromagnetic component, displaying hysteresis, is also present. It seems that the magnetic coupling between the intrasite irons is ferromagnetic while the intersite sublattices are coupled antiferromagnetically. The small ferromagnetic component observed in Fig. 12 may be due to an unequal iron concentration in the two sites (shared with cobalt). A difference of ~0.2% in the concentration is enough to explain the observed ferromagnetic component. Alternatively a very small canting (only ~0.2°) of the moments in the antiferromagnetic structure may also produce the observed ferromagnetic component.

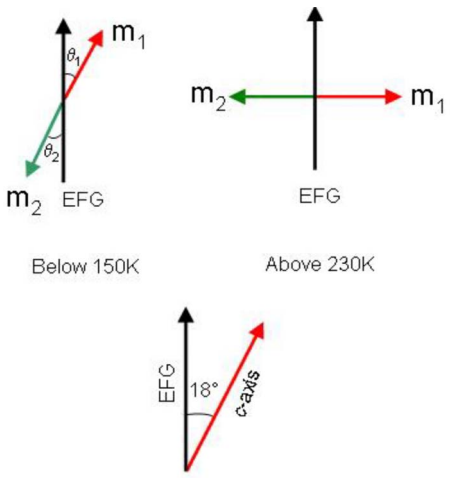

FIG. 10. (Color online) A schematic diagram of the relative alignment of two site moments with respect to the EFG and the crystallographic c axis.

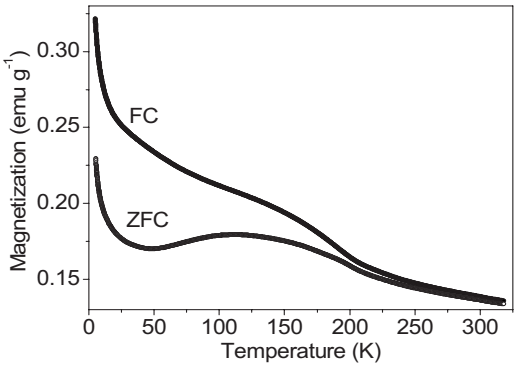

FIG. 11. The temperature dependence of the field cooled and zero field cooled magnetizations of Ca_3CoFeO_6 in 1 T.

Here it may be noted that the magnetic properties of Ca_3CoFeO_6 are very much different from that of the isostructural compound Ca_3CuMnO_6.[16] For the Ca_3CuMnO_6, two transitions for long-range magnetic ordering (not a common feature in a quasi-one-dimensional system), one at 5.5 K and other below 3.6 K, have been reported in the literature.[16] The transition at 5.5 K has been ascribed due to the antiferromagnetic ordering. Recently, the magnetic and electronic properties of Ca_3FeRhO_6 (Ref. 17) with the chemical formula similar to the present compound Ca_3FeCoO_6 but with a crystal structure like that of $Ca_3Co_2O_6$ have been studied. It was found that the ordering temperature of Ca_3FeRhO_6 is only $T_N=20$ K. The iron occupies the trigonal prism site, similar to the iron doped $Ca_3Co_2O_6$ and an equal strength of quadrupole interaction for both Ca_3FeRhO_6 and Ca_3FeCoO_6 has been found in the Fe Mössbauer study. These similarities and differences between the two compounds Ca_3FeRhO_6 and

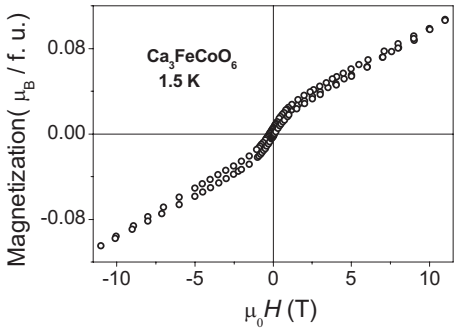

FIG. 12. Magnetic field dependence of the Ca_3FeCoO_6 magnetization at 1.5 K.

Ca_3FeCoO_6 prove that the local oxygen environment of Fe in the two compounds is very similar; however, due to the different crystal structure, the Fe-Fe exchange interactions are very different, T_N observed to be approximately 20 and 500 K for Ca_3FeRhO_6 and Ca_3FeCoO_6, respectively.

IV. CONCLUSIONS

Our Mössbauer studies of the iron doped $Ca_3(Co_{1-x}Fe_x)_2O_6$ compounds reveal that for $x \leqslant 0.2$ the iron resides only in the Co2 site. These compounds show paramagnetic behavior at 90 K and the iron exhibits slow spin relaxation phenomena even at room temperature. For the $x=0.5$ compound, the crystal structure changes (from rhombohedral to triclinic), where the iron resides almost equally in two different crystallographic sites and it exhibits a very high magnetic ordering temperature, $T_N \sim 500$ K. At $T_{sr} \sim 193$ K a spin reorientation of the iron magnetic moments is observed. Below T_{sr}, the moments in the two sites are aligned along the crystallographic *c* axis, whereas above T_{sr} they are aligned in the basal *a-b* plane. The magnetic order is ferromagnetic within each iron site and antiferromagnetic between the sites. A small ferromagnetic component observed in the magnetization studies is probably due to a very small difference in the occupation of the two iron sites. The unique magnetic properties of Ca_3CoFeO_6 ($x=0.5$) compare to the compounds with lower *x* values, or Ca_3FeRhO_6, are due to its different crystal structure, which may have some importance for its practical applications.

ACKNOWLEDGMENTS

I.N. gratefully acknowledges the support from the Israel Science Foundation (ISF, 2004 Grant No. 618/04).

[1] A. Jain, Sher Singh, and S. M. Yusuf, Phys. Rev. B **74**, 174419 (2006).
[2] K. E. Stitzer, J. Darriet, and H.-C. zur Loye, Curr. Opin. Solid State Mater. Sci. **5**, 535 (2001).
[3] S. Majumdar, V. Hardy, M. R. Lees, D. McK. Paul, H. Rousselière, and D. Grebille, Phys. Rev. B **69**, 024405 (2004).
[4] H. Kageyama, K. Yoshimura, K. Kosuge, M. Azuma, M. Takano, H. Mitamura, and T. Goto, J. Phys. Soc. Jpn. **66**, 3996 (1997).
[5] A. Maignan, C. Michel, A. C. Masset, C. Martin, and B. Raveau, Eur. Phys. J. B **15**, 657 (2000).
[6] S. Aasland, H. Fjellvåg, and B. Hauback, Solid State Commun. **101**, 187 (1997).
[7] V. Hardy, S. Lambert, M. R. Lees, and D. McK. Paul, Phys. Rev. B **68**, 014424 (2003).
[8] B. Martínez, V. Laukhin, M. Hernando, J. Fontcuberta, M. Parras, and J. M. González-Calbet, Phys. Rev. B **64**, 012417 (2001).
[9] B. Raquet, M. N. Baibich, J. M. Broto, H. Rakoto, S. Lambert, and A. Maignan, Phys. Rev. B **65**, 104442 (2002).
[10] R. Vidya, P. Ravindran, H. Fjellvåg, A. Kjekshus, and O. Eriksson, Phys. Rev. Lett. **91**, 186404 (2003).
[11] D. Flahaut, A. Maignan, S. Hébert, C. Martin, R. Retoux, and V. Hardy, Phys. Rev. B **70**, 094418 (2004).
[12] H. Kageyama, S. Kawasaki, K. Mibu, M. Takano, K. Yoshimura, and K. Kosuge, Phys. Rev. Lett. **79**, 3258 (1997).
[13] J. Arai, H. Shinmen, S. Takeshita, and T. Goko, J. Magn. Magn. Mater. **272-276**, 809 (2004).
[14] I. Nowik and H. H. Wickman, Phys. Rev. Lett. **17**, 949 (1966).
[15] J. Rodríguez-Carvajal, in *FULLPROF: A Program for Rietveld Refinement and Pattern Matching Analysis*, Abstracts of the Satellite Meeting on Powder Diffraction of the XV Congress of the IUCr, Toulouse, France, 1990, p. 127.
[16] K. Sengupta, S. Rayaprol, K. K. Iyer, and E. V. Sampathkumaran, Phys. Rev. B **68**, 012411 (2003).
[17] V. Eyart, U. Schwingenschlögl, R. Fresard, A. Maignan, C. Martin, N. Nguyen, C. Hackenberger, and T. Kopp, Phys. Rev. B **75**, 115105 (2007).